Electronic structure of $CeRhSn_2$ and $LaRhSn_2$ from x-ray photoemission spectroscopy and band structure calculations

2008 J. Phys.: Condens. Matter 20 025201

(http://iopscience.iop.org/0953-8984/20/2/025201)

IOP PUBLISHING JOURNAL OF PHYSICS: CONDENSED MATTER

J. Phys.: Condens. Matter **20** (2008) 025201 (8pp) doi:10.1088/0953-8984/20/02/025201

Electronic structure of $CeRhSn_2$ and $LaRhSn_2$ from x-ray photoemission spectroscopy and band structure calculations

M Gamża[1], A Ślebarski[1] and H Rosner[2]

[1] Institute of Physics, University of Silesia, 40-007 Katowice, Poland
[2] Max Planck Institute for Chemical Physics of Solids, D-01187 Dresden, Germany

E-mail: andrzej.slebarski@us.edu.pl and rosner@cpfs.mpg.de

Received 1 August 2007, in final form 1 October 2007
Published 6 December 2007
Online at stacks.iop.org/JPhysCM/20/025201

Abstract

We report on the electronic structure and magnetic properties of the Kondo lattice system $CeRhSn_2$ and of the reference compound $LaRhSn_2$. The Ce 3d and 4d x-ray photoemission spectroscopy (XPS) data point to a stable configuration of the Ce 4f shell in $CeRhSn_2$. The ac magnetic susceptibility measurements reveal two magnetic transitions for $CeRhSn_2$ at temperatures $T_{C1} \approx 4$ K and $T_{C2} \approx 3$ K. The temperature dependences of the ac susceptibility show also broad maxima at about 17 and 15 K for $CeRhSn_2$ and $LaRhSn_2$, respectively. Such features hint at spin fluctuations on Rh atoms. To get detailed insight into the electronic structure of both $CeRhSn_2$ and $LaRhSn_2$ we perform *ab initio* band structure calculations within the local (spin) density approximation (L(S)DA) and using the LSDA + U approach to account for the strong Coulomb interactions within the Ce 4f shell. The LSDA + U approximation gives qualitatively the correct physical picture of Ce^{3+} in $CeRhSn_2$. The reliability of the theoretical results is confirmed by the comparison of the calculated XPS valence band spectra with experimental data. A Fermi surface analysis shows that there are some parallel sections of the sheets, which could generate 'nesting' instabilities. These nesting features might be responsible for the spin fluctuations suggested by the ac susceptibility measurements.

(Some figures in this article are in colour only in the electronic version)

1. Introduction

Many Ce-based intermetallics exhibit a variety of unusual ground states, including complex magnetic structures, heavy fermion states (both normal and superconducting), magnetic Kondo lattices with reduced magnetic moments or non-magnetic insulating Kondo lattices. The reason for such a diversity of physical phenomena is a delicate interplay between two competing mechanisms: the local on-site Kondo screening of the localized Ce moments and the long range Ruderman–Kittel–Kasuya–Yosida (RKKY) interactions. The first effect suppresses the Ce 4f magnetic moments and may lead to the Abrikosov–Suhl resonance manifesting itself as the narrow peak in a quasi-particle density of states (DOS) near the Fermi level, while the latter one may lead to long range magnetic order of the localized Ce moments. Finally, the stability of different ground states depends strongly on the on-site hybridization strength between the 4f electrons and the conduction band, the bare f level position in the conduction band, the number of electrons occupying the f shell and the magnitude of on-site Coulomb interaction within this shell. The full understanding, however, of the relation between band structure and the ground state properties in Ce-based intermetallics still requires much further investigation.

Over the past few years, much attention has been devoted to magnetically ordered Kondo lattice compounds. Some of them were found to undergo a superconducting transition with applied pressure via a heavy fermion state [1–4]. The magnetic interactions are believed to play an essential role in the formation of the Cooper pairs in this superconducting state.

Table 1. Comparison of the structural data from experiment and LDA calculations for $CeRhSn_2$ and $LaRhSn_2$. The calculated lattice parameters and internal positions were rounded to two and three significant digits, respectively.

Lattice parameters for:	$LaRhSn_2$			$CeRhSn_2$		
	a	*b*	*c*	*a*	*b*	*c*
Experimental	4.637	17.108	9.642	4.600	17.000	9.594
Experimental [5]	4.639	17.100	9.637	4.603	17.029	9.613
Experimental [6]	—	—	—	4.5929	16.9849	9.5896
Theoretical (LDA)	4.58	17.11	9.57	4.52	16.92	9.44
Atomic positions						
Atom	Wyckoff site	*x*	*y*	*z*		
RE1	4c	0	y_{RE1}	0.25		
RE2	4b	0	0.5	0		
Rh	8f	0	y_{Rh}	z_{Rh}		
Sn1	8f	0	y_{Sn1}	z_{Sn1}		
Sn2	4c	0	y_{Sn2}	0.25		
Sn3	4c	0	y_{Sn3}	0.25		
Compound:	$LaRhSn_2$		$CeRhSn_2$			
	Experiment [5]	LDA	Experiment [5]	LDA		
y_{RE1}	0.2976	0.297	0.295 65	0.297		
y_{Rh}	0.1485	0.146	0.146 62	0.145		
z_{Rh}	0.5069	0.507	0.504 64	0.508		
y_{Sn1}	0.3039	0.302	0.302 08	0.301		
z_{Sn1}	0.5889	0.591	0.589 74	0.591		
y_{Sn2}	0.0921	0.092	0.091 25	0.090		
y_{Sn3}	0.9277	0.929	0.926 29	0.928		

Since there are not many magnetically ordered Kondo lattice compounds and the mechanism leading to formation of the unconventional superconducting ground state in some of them is not well explained yet, it is of great importance to investigate in detail the electronic structure of this type of compounds.

In this paper, we present a study of the electronic structure of $CeRhSn_2$ and of the reference system $LaRhSn_2$. The compound $CeRhSn_2$ was found to be a Kondo lattice system which undergoes a magnetic phase transition at a temperature of 4 K [5]. Magnetization data suggested the presence of a metamagnetic transition [6]. We performed x-ray photoelectron spectroscopy (XPS) measurements to investigate the valence of Ce ions in the compound $CeRhSn_2$. Basing on the Gunnarsson–Schönhammer theoretical model [7] we estimate the hybridization energy between the Ce 4f shell and the conduction band states. The XPS valence band spectrum we compare and interpret in terms of *ab initio* band structure calculations performed using the full potential local orbital minimum basis band structure (FPLO) code [8]. To investigate in detail the character of Ce 4f states in $CeRhSn_2$ and their influence on the other valence band states we draw a parallel between the experimental and theoretical results for both $CeRhSn_2$ and the reference compound $LaRhSn_2$. We also carry out ac magnetic susceptibility measurements down to a temperature of 2 K to get insight into the low temperatures magnetic properties. Finally, we are looking for indications which could explain the origin of the low temperature magnetic fluctuations suggested by the ac magnetic susceptibility results.

2. Methods

2.1. Experimental details

Polycrystalline samples of $CeRhSn_2$ and $LaRhSn_2$ were prepared by arc melting of the elemental metals (Ce 99.99%, La 99.99%, Rh 99.95%, Sn 99.995%, in units of atomic %) in the ratio 1:1:2 on a water cooled cooper hearth in an ultrahigh purity Ar atmosphere with an Al getter (heated above the melting point). Both samples were re-melted several times to promote homogeneity and annealed at 800 °C for 7 days. The quality of the samples was examined by the x-ray powder diffraction (XRD) analysis. The measurements were performed on a Siemens D-5000 diffractometer using Cu Kα radiation. The XRD pattern analysis revealed that both compounds crystallize in an orthorhombic structure (space group: *Cmcm*), consistent with previous results [5]. The lattice parameters acquired from the diffraction patterns analysis (table 1) are in agreement with those previously reported [5, 6]. The sample $LaRhSn_2$ was found to consist of a single phase, while for $CeRhSn_2$ a few additional low intensity Bragg peaks were detected, which originate from an unidentified minority phase. The energy dispersive x-ray spectroscopy (EDXS) microanalysis is performed to investigate in detail the composition of the $CeRhSn_2$ samples and their homogeneity. The quantitative measurements were carried out at several points on the polished surface. The composition of the main phase is found to be $Ce_{1\pm0.05}Rh_{0.99\pm0.04}Sn_{2.04\pm0.07}$, in agreement with stoichiometric $CeRhSn_2$. We also detected a few small grains of a secondary phase in an amount smaller than 5% of the bulk $CeRhSn_2$ sample, which is consistent

with the XRD analysis. The polarized light patterns as well as the XRD spectra analysis revealed that there is a preferred orientation of both polycrystalline samples, in agreement with previous reports [6].

The XPS spectra were obtained with monochromatized Al Kα radiation at room temperature using a PHI 5700 ESCA spectrometer. Total energy resolution was about 0.4 eV. Polycrystalline samples were broken under a high vacuum of 6×10^{-10} Torr immediately before taking spectra. Calibration of the spectra was performed according to [9]. Binding energies were referenced to the Fermi level ($\epsilon_F = 0$).

The ac magnetic susceptibility was measured in the temperature range of 1.8–300 K using a commercial ac Lake-Shore susceptometer. The amplitude of the excitation field was 1 mT at a fixed frequency of 10 kHz.

2.2. Computational

The electronic structure of both $CeRhSn_2$ and $LaRhSn_2$ compounds is studied by the full potential local orbital (FPLO) minimum basis method [8] within the local (spin) density approximation (L(S)DA). In the scalar relativistic calculations the exchange–correlation (XC) potential of Perdew and Wang was used [10]. The strongly correlated Ce 4f states in $CeRhSn_2$ were treated in mean field approximation within the LSDA + U approach [11] (applying the around mean field double-counting scheme) using an additional Coulomb repulsion U of 3–8 eV. The exchange constant J for the Ce 4f states was assumed to be 0–1 eV, according to [12].

Within this range of parameters, no significant changes of the electronic structure apart from the exact positions of the Ce 4f levels were observed. As the basis set, Ce(4f, 5s, 5p, 5d, 6s, 6p), La(5s, 5p, 5d, 6s, 6p, 4f), Rh(4s, 4p, 4d, 5s, 5p) and Sn(4s, 4p, 4d, 5s, 5p, 5d) states were employed. The lower lying states were treated fully relativistically as core states. The La 4f and Sn 5d states were taken into account as polarization states to increase the completeness of the basis set. The Ce(4f, 5s, 5p), La(5s, 5p), Rh(4s, 4p) and Sn(4s, 4p, 4d) states were treated as semi-core states to account for non-negligible core–core overlaps. The spatial extension of the basis orbitals was optimized to minimize the total energy [13]. A k-mesh of 64 points in the irreducible part of the Brillouin zone (294 in the full zone) was used.

On the basis of the band structure results we calculated the theoretical XPS valence band spectra. The partial l-resolved densities of states were multiplied by the corresponding cross sections [14] and convoluted by the Lorentzians with a full width at half-maximum of 0.4 eV to account for the instrumental resolution, thermal broadening and the effect of the lifetime of the hole states. The results were convoluted with the Fermi–Dirac function for 300 K.

3. Results and discussion

3.1. XPS results

Ce core level photoemission is an appropriate tool for getting insight into the character of the Ce 4f states in Ce-based intermetallics owing to the strong Coulomb interaction between the photoemission core hole and the electrons near the Fermi level. This coupling results in a complex structure of the Ce core level XPS spectra.

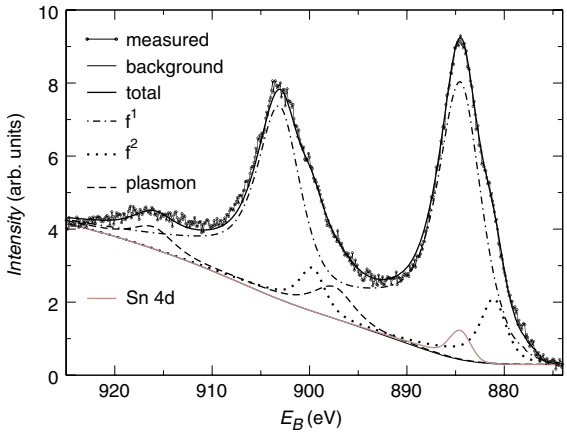

Figure 1. The Ce 3d XPS spectrum of $CeRhSn_2$ deconvoluted based on the Gunnarsson and Schönhammer theoretical model [7].

Figure 1 shows the Ce 3d XPS spectrum of $CeRhSn_2$. A background, calculated using the Tougaard algorithm [15], was subtracted from the XPS data. The separation of the overlapping peaks in the spectrum was done on the basis of the Doniach–Šunjić theory [16]. The spin–orbit (SO) interaction results in two sets of Ce 3d photoemission lines in the spectrum, which are assigned to the $3d_{3/2}$ and $3d_{5/2}$ components of the final states, with intensity ratio $I(3d_{5/2})/I(3d_{3/2}) = 3/2$. The estimated value of the SO splitting (δ) equals 18.6 eV. The *ab initio* band structure calculations gave a very similar result for the SO splitting ($\delta \approx$ 18.84 eV) for Ce atoms in $CeRhSn_2$ compound. Additionally, in the spectrum there is also a slight contribution originating from the Sn 3s states at the binding energy of 885 eV, which overlaps with the Ce 3d peaks.

Each SO set of the Ce 3d photoemission lines consists of contributions marked as f^0, f^1 and f^2. The main peaks $3d^9f^1$ originate from Ce^{3+}. The $3d^9f^2$ final state components appears when the core hole becomes screened by an additional 4f electron, which is possible due to the hybridization of the Ce 4f shell with the conduction band. Consequently, the contribution of the $3d^9f^2$ lines in the measured Ce 3d spectrum reflects the hybridization strength. The quantitative analysis was performed based on the Gunnarsson and Schönhammer (GS) theory [7]. The details of the method were described elsewhere [17]. For the hybridization energy Δ, which describes the hybridization part of the Anderson impurity Hamiltonian and reflects the hybridization strength between the Ce 4f shell and conduction band, we estimate about 85 meV for the compound $CeRhSn_2$.

It is worthwhile to stress that there are two crystallographic positions occupied by Ce atoms for the $CeRhSn_2$ compound and the measured Ce XPS spectra represent the total signal from all contributions of Ce atoms. The Ce atoms in nonequivalent positions have different local environments, which could lead to the different chemical shifts of their photoemission lines. However, from the *ab initio* band structure

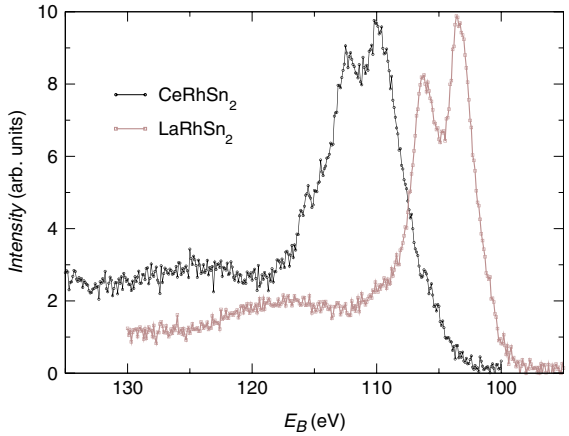

Figure 2. The Ce 4d XPS spectra of $CeRhSn_2$ and $LaRhSn_2$.

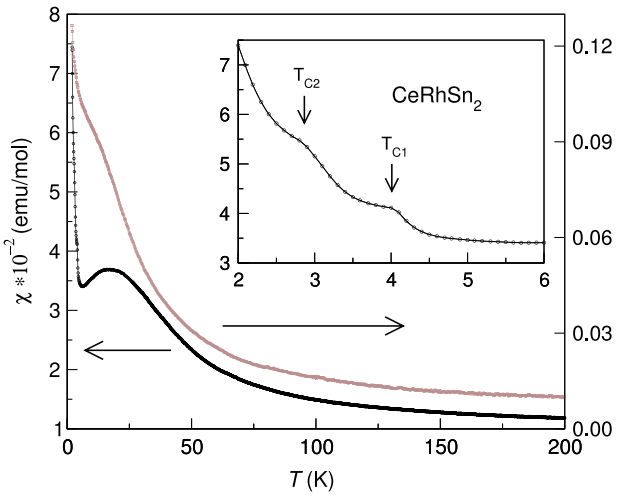

Figure 3. The ac magnetic susceptibility of $CeRhSn_2$ (black line with scale on the left side) and of the reference $LaRhSn_2$ (grey (brown) line with scale on the right side). The inset shows the low temperature part of the susceptibility for $CeRhSn_2$ with two magnetic phase transitions marked as T_{C1} and T_{C2}.

calculations we found that the differences in binding energy between two different types of Ce atoms are of the order of 0.1–0.3 eV, depending on the applied approximation (LDA, LSDA, LSDA + U). These shifts are much smaller than the intervals between the f^1 and f^2 final state contributions in Ce 3d XPS spectrum. This allows us to interpret the estimated Δ value as the *average* hybridization energy for both types of Ce atoms in $CeRhSn_2$.

In the Ce 3d XPS spectrum of $CeRhSn_2$ we found also additional contributions at the binding energies of 897 and 915.6 eV. We interpret them as plasmons arising from group oscillations of the conduction electrons, since in the La 3d XPS spectrum of $LaRhSn_2$ similar plasmon-like features were found. For both spectra the plasmon energy, i.e. the energy interval between the main peak and the loss line, was found to be about 12.5 eV. We did not find any additional, sharp peaks in the Ce 3d XPS spectrum in a similar energy range which would provide evidence of a mixed valence of Ce. This result is consistent with magnetic susceptibility measurements [5], which indicated that at the room temperature the effective magnetic moment calculated per Ce atom is close to that expected for Ce^{3+}.

The stable valence of the Ce ions in $CeRhSn_2$ has also been confirmed by the Ce 4d XPS spectrum (figure 2), where one can observe only a multiplet structure of the binding energies ranging between 104 and 116 eV. These lines are assigned to the $3d^9f^1$ final state. There is no clear evidence for additional peaks at the higher binding energy, which could be attributed to the Ce $3d^9f^0$ state [18]. In the Ce 4d XPS spectrum one can find only a wide plasmon-like feature located at about 125 eV. An analogous contribution is visible in the La 4d spectrum for $LaRhSn_2$ (figure 2).

We have collected also the XPS valence band spectra for both $CeRhSn_2$ and $LaRhSn_2$ compounds. Their interpretation in terms of the theoretical band structure results is discussed in section 3.3.

3.2. Magnetic susceptibility

To get insight into the low temperature properties of the compound $CeRhSn_2$ we performed the ac magnetic susceptibility measurements down to 2 K. The temperature dependence of the ac susceptibility for $CeRhSn_2$ is shown in figure 3. There are two features visible in the low temperature part of the susceptibility curve at about 4 and 3 K, giving clear evidence for magnetic phase transitions. This result is in agreement with previous reports, which pointed to the complicated magnetic phase diagram with a first magnetic transition at $T_{C1} \approx 4$ K [5]. The second phase transition at $T_{C2} \approx 3$ K was suggested from the low field dc magnetization data [6]. In addition, the temperature dependence of the ac susceptibility shows a broad maximum at about 17 K. We assign this feature to spin fluctuation effects.

To investigate the origin of the feature observed in $CeRhSn_2$, we performed also ac magnetic susceptibility measurements for the $LaRhSn_2$ compound (see figure 3). For the reference system we find a broad maximum in the susceptibility curve at about 15 K. For the two compounds the features were found at similar temperatures, suggesting that they are related to spin fluctuations of Rh 4d electrons, as was proposed previously also for the compound CeRhSn [19]. To get insight into the magnetic properties we performed band structure calculations.

3.3. Electronic band structure calculations

For both compounds studied we first performed a full crystal structure optimization within the LDA approximation. The experimental data [5] are taken as a starting point. The obtained lattice parameters and atomic coordinates are listed in table 1. We cross-checked the FPLO results with the WIEN2K computer code [20], in which the forces at the atoms were calculated according to the method proposed by Yu *et al* [25]. For the optimized atomic coordinates we got total forces on each atom smaller than 4 mRyd au^{-1} For $CeRhSn_2$; however, the slightly larger deviations can be understood due to the less accurate convergence caused by the flat Ce 4f bands near

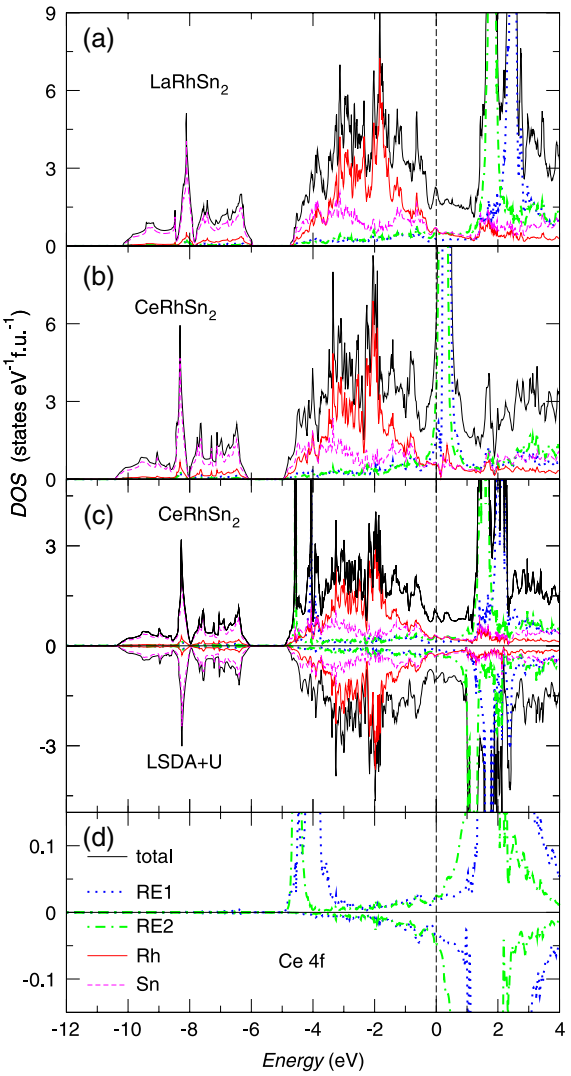

Figure 4. The total and atom-projected density of states of $LaRhSn_2$ (a) and $CeRhSn_2$ (b) calculated within the LDA approximation. Panel (c) presents the total and atomic-spin-resolve density of states of $CeRhSn_2$ calculated within the LSDA + U ($U = 6$ eV) approach applied for the Ce 4f shell. Panel (d) shows the resulting Ce 4f density of states for Ce atoms in both nonequivalent positions. The common vertical dashed line indicates the position of the Fermi level.

the Fermi level (figure 4). Nevertheless, the theoretical data are in good agreement with the experimental ones for both $CeRhSn_2$ and $LaRhSn_2$ suggesting that there is no significant contribution of the Ce 4f electrons to the chemical bonding.

Figure 4 shows the results of the calculations of the total and partial atom-resolved densities of states (DOS) for $CeRhSn_2$ and $LaRhSn_2$ within the LDA approximation. We performed also spin-polarized band structure calculations for both compounds (not shown). The results confirmed a magnetic ground state for $CeRhSn_2$, in agreement with the experimental findings. In contrast, for $LaRhSn_2$ the calculations yield a non-magnetic ground state. The theoretical results show that only the Ce atoms carry magnetic moments in the investigated compounds (table 2). The calculated spin

Table 2. DOS(ϵ_F), Sommerfeld coefficients γ and spin moments M of Ce1 and Ce2 calculated for the compounds $CeRhSn_2$ and $LaRhSn_2$ within different approximations for the XC potential.

Compound:	$LaRhSn_2$ LDA	$CeRhSn_2$ LDA	LSDA	LSDA + U ($U \sim 6$ eV)
DOS(ϵ_F) (states eV^{-1} f.u.$^{-1}$)	2.12	6.63	6.16	2.01
γ (mJ mol^{-1} K^{-2})	5.0	15.6	14.5	4.7
M_{RE1} (μ_B)	—	—	0.22	1.01
M_{RE2} (μ_B)	—	—	0.79	1.03

moments of Rh and Sn are very small in $CeRhSn_2$ (below 0.005 μ_B), while in $LaRhSn_2$ spin polarization is not observed.

The XPS core level spectra as well as magnetic susceptibility data [5] revealed that the Ce atoms have a stable trivalent configuration in $CeRhSn_2$, suggesting the strongly correlated character of the Ce 4f states. In contrast, in the L(S)DA calculations the partial Ce1 and Ce2 4f DOSs form unrealistic peaks at the Fermi level because of the large underestimation of the Coulomb repulsion of the f electrons within the L(S)DA approximation. In order to account for the strong Coulomb interaction within the Ce 4f shell we carried out band structure calculations using the so-called LSDA + U approach (figure 4). Inclusion of the Hubbard-type correlation term U to the XC potential shifts the occupied Ce 4f band towards higher binding energy and the unoccupied 4f states above the Fermi level. Consequently, it removes the incorrect hybridization with conduction states and yields the qualitatively correct physical picture of Ce^{3+} states. Thus, the magnetic spin moments are about 1 μ_B for the Ce atoms in both nonequivalent positions and the occupied and unoccupied Ce 4f states show a split of the order of U.

The typical U value for Ce in a trivalent state was found to be about 5–7 eV. Consistent results were obtained using the separation of the core level peaks in XPS and the f^2 peak in bremsstrahlung isochromat spectroscopy [21, 22] as well as basing on theoretical estimates [23, 24]. We note that a similar value of the U parameter was suggested recently for Ce in another magnetically ordered Kondo lattice compounds [26].

We varied the value of the U parameter in a range of 3–8 eV, for both types of Ce atoms in $CeRhSn_2$. In the investigated range of U values the shape of the electronic DOS for all atoms except Ce almost does not depend on the U value. What is more, the dependence on the chosen U value is negligible in the region around the Fermi level that is relevant for the low lying excitations. This justifies the application of the LSDA + U approximation, although the real value of the U parameter may vary slightly for the Ce atoms in both nonequivalent positions.

Magnetic spin moments on Rh and Sn obtained within the LSDA + U approximation are below 0.01 μ_B, indicating that only Ce atoms carry a magnetic moment in th $CeRhSn_2$ compound. Hence, in a first approximation, magnetic ordering in $CeRhSn_2$ can be explained as due to the RKKY type interactions among the rather localized Ce 4f states, that couple via the itinerant electrons.

The calculated values of the DOS at the Fermi level and Sommerfeld coefficients γ are listed in table 2. The theoretical γ values for $CeRhSn_2$ are much lower than that estimated from the fit of the low temperature specific heat data (300 mJ mol^{-1} K^{-2}) [6]. However, one should keep in mind that the LSDA + U method is a mean field approximation, which can be considered only as the first step toward a better description of strongly correlated electron systems. All dynamic correlation effects are neglected in this approach and would require a more sophisticated theoretical treatment. The strong enhancement of the gamma coefficient for $CeRhSn_2$ could result from electronic contributions, thus suggesting the formation of the Abrikosov–Suhl resonance near the Fermi level, or it could be partly due to the low lying magnetic excitations.

It is worthwhile to stress that the assumption of strong Coulomb interaction within the Ce 4f shell results in occupied 4f states forming narrow peaks below the Fermi level, but there is still some contribution of these states near the Fermi level due to the hybridization with conduction band states (see figure 4). This residual tiny 4f contribution in a region of the low binding energies is similar to the 4f contributions of La1 and La2 in $LaRhSn_2$, slightly larger for RE1 than for RE2 in both compounds. This might indicate that Ce1 contributes more to the formation of the experimentally observed Kondo lattice state [6].

To check the reliability of the numerical results we calculated the theoretical XPS valence band spectra according to the description in section 2.2 and compare them with the experimental data (figure 5). The main peaks in the valence XPS spectra for $LaRhSn_2$ and for $CeRhSn_2$ originate to large extent from the Sn 5p states hybridized with 4d states of Rh. The second peaks centred at about 8 eV originate mainly from the Sn 5s states. However, for the investigated compounds the Sn atoms occupy three nonequivalent positions. Our band structure results indicate that states of Sn1, Sn2 and Sn3 atoms strongly hybridize with each other forming common bands. This explains why ^{119}Sn Mössbauer measurements [5] resulted in spectra with only slightly enlarged linewidth, despite the signal coming from three different Sn sites.

Direct comparison of the $CeRhSn_2$ and $LaRhSn_2$ XPS valence band spectra (figure 5(a)) shows that there is no significant difference in their shape. Subtraction of the $LaRhSn_2$ valence band spectrum from that of $CeRhSn_2$ has revealed that there are only very slight differences between these two spectra in a range of binding energies of 2–4.5 eV (figure 5(b)), which might originate from the Ce 4f states. Our band structure calculations shown that the occupied Ce 4f states are located within this energy range assuming that the U parameter takes values of 4–6 and 3–5 eV for Ce1 and Ce2, respectively. To illustrate the Ce 4f contributions to the XPS valence band spectrum we plotted the partial Ce 4f DOSs as well as the sum of all partial l-resolved DOSs, multiplied by the corresponding cross sections, calculated for $CeRhSn_2$ within the LDA and LSDA + U (U = 6 eV) approximations (figures 5(d) and (e)). It is clearly visible that the Ce 4f states give only a small contribution to the XPS valence band spectrum of $CeRhSn_2$, in agreement with the experimental results. Therefore, the XPS valence band spectra cannot give unequivocal information about the Ce 4f states in $CeRhSn_2$. It is worthwhile to stress, however, that the shape of the all partial densities of states as well as the band structure, except for the 4f bands, are very similar for $LaRhSn_2$ and $CeRhSn_2$ with the Ce 4f shell treated within the LSDA + U approach. This gives strong support for the picture that Ce 4f states are well localized in $CeRhSn_2$.

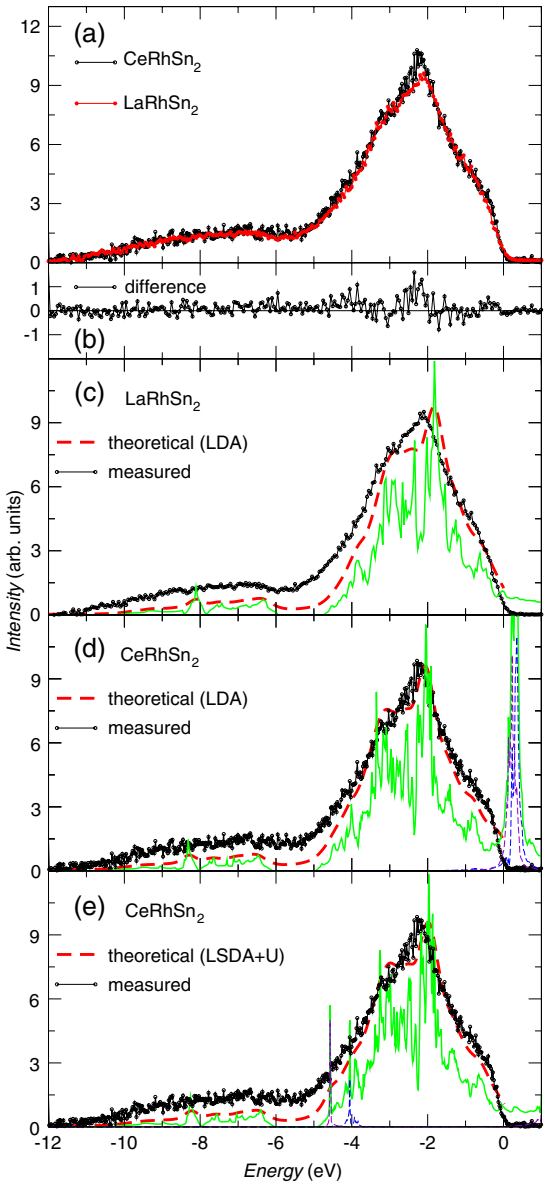

Figure 5. The XPS valence band spectra of $CeRhSn_2$ and of $LaRhSn_2$ (a) and their difference (b). In panels (c), (d) and (e), the XPS valence band spectra of $LaRhSn_2$ and $CeRhSn_2$ (background subtracted), are compared with the calculated ones based on the FPLO densities of states within the LDA approximation and using the LSDA + U (U = 6 eV) approach for the strong Coulomb interactions within the Ce 4f shell for $CeRhSn_2$. The thin grey (green) solid lines represent the sum of the partial l-resolved DOSs multiplied by the corresponding cross sections. The thin dashed dark grey (blue and violet) lines show the partial Ce1 and Ce2, respectively, 4f DOSs is multiplied by the photoemission cross section.

Finally, we would like to discuss indications which provide insight into the possible origin of the spin fluctuations on Rh in $LaRhSn_2$ and $CeRhSn_2$ suggested by the ac magnetic susceptibility data. Even for the $CeRhSn_2$ compound our band structure results did not show any localized magnetic moment on Rh atoms. This is in agreement with a simple picture based on the molecular orbital scheme. In this formulation, the Rh atoms in $CeRhSn_2$ are expected to have a d^6 configuration which is non-magnetic for the resulting low spin state [5]. On the other hand, the numerically calculated Rh DOS(ϵ_F) is smaller than one state per eV and atom. A crude estimation (assuming the exchange integral for Rh 4d states to be of the order of 0.5) shows that in this case the Stoner criterion for band magnetism is not fulfilled. Fixed spin moment (FSM) calculations for $LaRhSn_2$ also do not give evidence for ferromagnetic spin fluctuations in this compound. To investigate in detail indications of magnetic instabilities we performed a Fermi surface analysis for $LaRhSn_2$. The $CeRhSn_2$ bands in the vicinity of the Fermi level are very similar to those of the $LaRhSn_2$ system causing topologically identical Fermi surfaces. Thus, we show only the results for $LaRhSn_2$. We find that the Fermi surface of this compound consists of five different sheets. Four of them are presented in figure 6, while the fifth one is similar to a free-electron sheet. The most interesting features are the parallel 'pieces' of the sheet presented in figure 6(b), which could generate 'nesting' instabilities. Since there is a significant contribution of Rh states to these Fermi surface sections, these nesting features might be the origin for the spin fluctuations suggested by the ac susceptibility measurements.

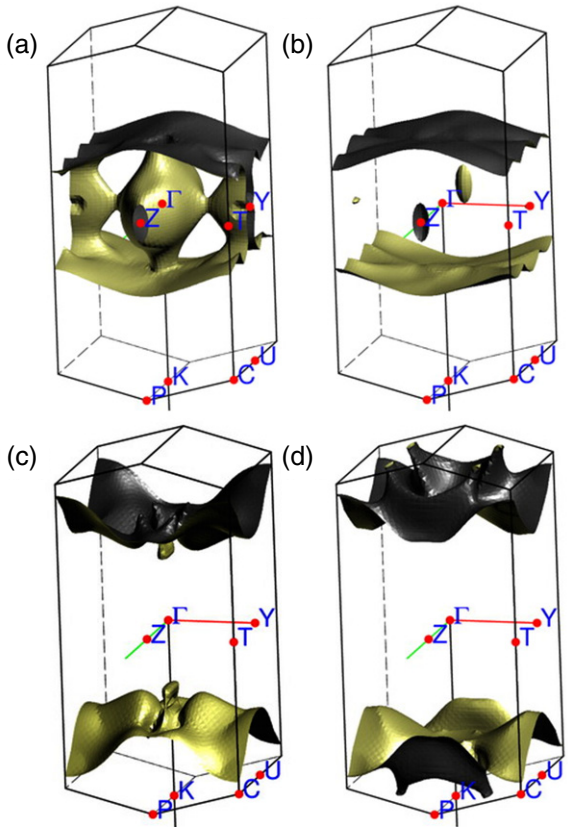

Figure 6. Four sheets of the Fermi surface of $LaRhSn_2$. The high symmetry points are labelled according to the standard notation.

4. Concluding remarks

We investigated the electronic structure and magnetic properties of the Kondo lattice system $CeRhSn_2$ and of the reference compound $LaRhSn_2$. The main part of our studies involved the nature of the Ce 4f states in the $CeRhSn_2$ system. The Ce 3d and 4d XPS spectra point to a stable configuration of the Ce 4f shell, in agreement with magnetic susceptibility measurements [5]. The energy of hybridization, Δ, between the Ce 4f states and conduction band states was estimated to be about 85 meV. This value could be interpreted as the *average* hybridization energy for Ce atoms occupying two nonequivalent positions. The XPS valence band spectra for $CeRhSn_2$ and $LaRhSn_2$ we analysed in terms of *ab initio* band structure calculations.

The theoretical results indicate that there is no significant contribution of the Ce 4f electrons to the chemical bonding in $CeRhSn_2$. We have found that the LSDA + U approximation provides the qualitatively correct physical picture of Ce^{3+} states in $CeRhSn_2$. Moreover, the electronic structure of this compound calculated within the LSDA + U approach is very similar to that of the reference compound $LaRhSn_2$, which in comparison with the XPS spectra indicates that Ce 4f states are well localized in $CeRhSn_2$.

The ac magnetic susceptibility measurements revealed two magnetic transitions for $CeRhSn_2$ at temperatures $T_{C1} \approx 4$ K and $T_{C2} \approx 3$ K, suggesting a more complicated magnetic phase diagram. The temperature dependences of the ac susceptibilities show also broad maxima at about 17 and 15 K for $CeRhSn_2$ and $LaRhSn_2$, respectively, suggesting spin fluctuations of Rh 4d electrons in both compounds.

The Fermi surface analysis performed for both compounds shows that there are some parallel sections of the sheets, which might generate 'nesting' instabilities and be responsible for the spin fluctuation effects. Obviously, further experimental studies (e.g. neutron scattering experiments) should be carried out to improve the understanding of the magnetic properties of the compounds $CeRhSn_2$ and $LaRhSn_2$.

Acknowledgments

The authors thank Ulrich Burkhardt for sample characterization and Jerzy Kubacki for help with XPS experiments. The authors are also grateful for financial support from Projects No 1 P03B 052 28, No N202 010 32/0487 of Ministry of Science and Higher Education and for the DFG Emmy Noether programme.

References

[1] Mathur N D, Grosche F M, Julian S R, Walker I R, Freye D M, Haselwimmer R K W and Lonzarich G G 1998 *Nature* **394** 39

[2] Movshovich R, Graf T, Mandrus D, Thompson J D, Smith J L and Fisk Z 1996 *Phys. Rev.* B **53** 8241

[3] Walker I R, Grosche F M, Freye D M and Lonzarich G G 1997 *Physica* C **282** 303
[4] Grosche F M, Walker I R, Julian S R, Mathur N D, Freye D M, Steiner M J and Lonzarich G G 2001 *J. Phys.: Condens. Matter* **13** 2845
[5] Niepmann D, Pöttgen R, Künnen B, Kotzyba G, Rosenhahn C and Mosel B D 1999 *Chem. Mater.* **11** 1597
[6] Hossain Z, Gupta L C and Geibel C 2002 *J. Phys.: Condens. Matter* **14** 9687
[7] Gunnarsson O and Schönhammer K 1983 *Phys. Rev.* B **28** 4315
[8] Koepernik K and Eschrig H 1999 *Phys. Rev.* B **59** 1743
[9] Baer Y, Bush G and Cohn P 1975 *Rev. Sci. Instrum.* **46** 466
[10] Perdew J P and Wang Y 1992 *Phys. Rev.* B **45** 13244
[11] Eschrig H, Koepernik K and Chaplygin I 2003 *J. Solid State Chem.* **176** 482
[12] Boring A M, Albers R C, Eriksson O and Koelling D D 1992 *Phys. Rev. Lett.* **68** 2652
[13] Eschrig H 1989 *Optimized LCAO Method and the Electronic Structure of Extended Systems* (Berlin: Springer)
[14] Yeh J J and Lindau J 1985 *At. Data Nucl. Data Tables* **32** 1
[15] Tougaard S and Sigmund P 1982 *Phys. Rev.* B **25** 4452
[16] Doniach S and Šunjić M 1970 *J. Phys. C: Solid State Phys.* **3** 286
[17] Ślebarski A, Zawada T, Spałek J and Jezierski A 2004 *Phys. Rev.* B **70** 235112
[18] Fuggle J C, Hillebrecht F U, Zolnierek Z, Lässer R, Freiburg Ch, Gunnarsson O and Schönhammer K 1983 *Phys. Rev.* B **27** 7330
Signorelli A J and Hayes R G 1973 *Phys. Rev.* B **8** 81
[19] Ślebarski A, Spałek J, Gamża M and Hackemmer A 2006 *Phys. Rev.* B **73** 205115
[20] Blaha P, Schwarz K, Madsen G, Kvasnicka D and Luitz J 2001 *Program for Calculating Crystal Properties WIEN2k* Vienna University of Technology (ISBN 3-9501031-1-2)
[21] Baer Y, Ott H R, Fuggle J C and De Long L E 1981 *Phys. Rev.* B **24** 5384
[22] Lang J K, Baer Y and Cox P A 1981 *J. Phys. F: Met. Phys.* **11** 121
[23] Herbst J F, Watson R E and Wilkins J W 1978 *Phys. Rev.* B **17** 3089
Herbst J F and Wilkins J W 1979 *Phys. Rev. Lett.* **43** 1760
[24] Anisimov V I and Gunnarsson O 1991 *Phys. Rev.* B **43** 7570 and references there in
[25] Yu R, Singh D and Krakauer H 1991 *Phys. Rev.* B **43** 6411
[26] Krellner C, Brüning E M, Koch K, Rosner H, Nicklas M, Baenitz M and Geibel C 2007 *Phys. Rev.* B **76** 104418